PtFeCoNiMo high-entropy alloy nanocatalysts for high-performance alkaline hydrogen evolution

Xiaolong Ma*, Song Hu, Jiaqin Wang, Guochang Lv, Yuxue Hu, Yu Xiao, Gang Hu* and Biao Qin*

School of Chemistry and Chemical Engineering, Zunyi Normal University, Zunyi, Guizhou 563006, China

*Corresponding Author.

E-mail address: shawnma1990@163.com

Calculation of the configurational ΔS_{mix}, ΔH_{mix}, and ΔG_{mix}

The configuration entropy ((ΔS_{mix}) of multi-element alloys increases with the number of different kinds of cations. The calculation of ΔS_{mix} can be performed by using the equation:

$$\Delta S_{mix} = -R\sum C_i InC_i \tag{1}$$

Where R is the gas constant and C_i is the mole fraction of each cation. According to the calculation of the ΔS_{mix}, alloys can be divided into low ((ΔS_{mix}< 1R), medium (1R ≤ (ΔS_{mix}≤ 1.5R), and HEAs (ΔS_{mix} > 1.5R)[1].

It is worth to note that the formation of a solid solution phase of high entropy alloy requires following conditions: atomic radius difference δ ≤ 6.6%, and the mixing enthalpy -11.6 ≤ΔH_{mix}≤ 3.2 kJ mol^{-1}. The atomic radius difference and mixing enthalpy can be calculated by using following equations:

$$\bar{r} = \sum_{i=1}^{n} C_i r_i \tag{2}$$

$$\delta = \sqrt{\sum iC_i\left(1 - \frac{r_i}{\bar{r}}\right)^2} \tag{3}$$

$$\Omega_{ij} = \Delta H_{ij}^{mix} \tag{4}$$

$$\Delta H_{mix} = \sum_{i=1\ i\neq j}^{n} \Omega_{ij} C_i C_j \tag{5}$$

where r is the average atomic radius in the alloy, r_i is the atomic radius of the i_{th} metallic element, ΔH_{mix} is the mixing enthalpy of the binary ij alloy[2]. The ΔG_{mix} can be calculated by using the equation:

$$\Delta G_{mix} = \Delta H_{mix} - T\Delta S_{mix} \tag{6}$$

Calculation of the turnover frequency (TOF)

The turnover frequency values were calculated by following equation:

$$TOF = jA/2Fn\ (HER) \tag{7}$$

in the given equation, " j " represents the current density at a specific overpotential, " A " stands for the surface area of the electrode, "2" represent the number of moles of electrons transferred to produce one mole of H_2 and O_2 respectively, " F " represents the Faraday constant (96,485 C mol^{-1}), and " n " represents the number of moles of active sites. The recorded TOFs were based on the assumption that the noble metal atoms present in the samples exhibit catalytic activity[3].

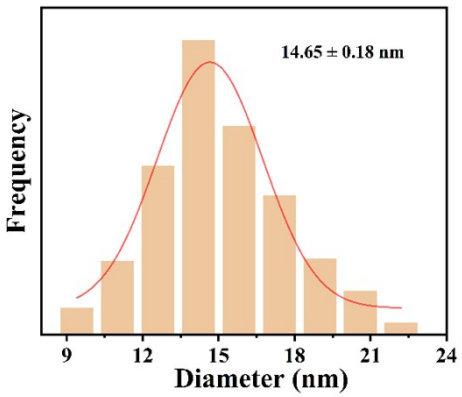

Figure S1. Particle size distribution of $Pt_{27}Fe_{30}Co_{27}Ni_9Mo_7/C$.

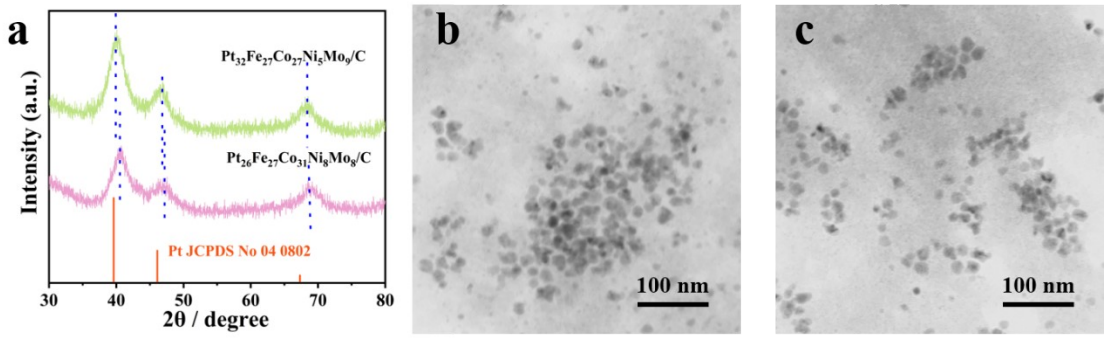

Figure S2. (a) XRD spectrum, and (b, c) TEM image of $Pt_{32}Fe_{27}Co_{27}Ni_5Mo_9/C$ and $Pt_{26}Fe_{27}Co_{31}Ni_8Mo_8/C$.

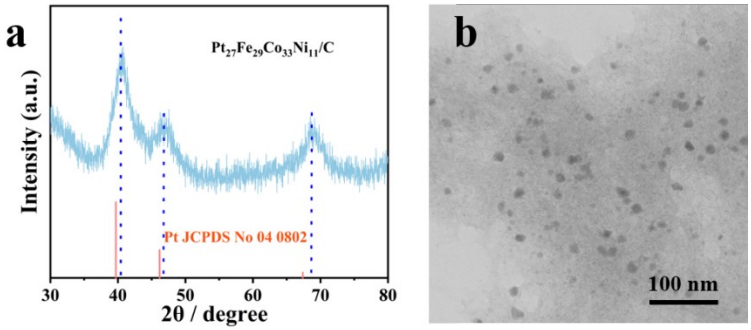

Figure S3. (a) XRD spectrum, and (b) TEM image of c.

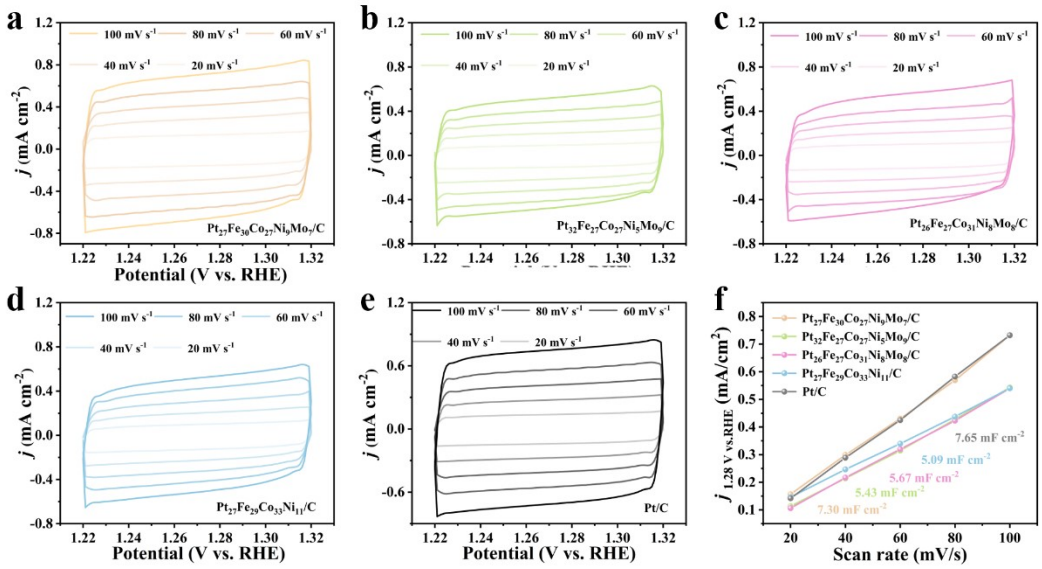

Figure S4. CV curves of (a) $Pt_{27}Fe_{30}Co_{27}Ni_9Mo_7/C$, (b) $Pt_{32}Fe_{27}Co_{27}Ni_5Mo_9/C$, (c) $Pt_{26}Fe_{27}Co_{31}Ni_8Mo_8/C$, (d) $Pt_{27}Fe_{29}Co_{33}Ni_{11}/C$, and (e) Pt/C in the double layer region at scan rates of 20, 40, 60, 80 and 100 mV s^{-1} in 1.0 M KOH. (f) The C_{dl} capacitance of catalysts.

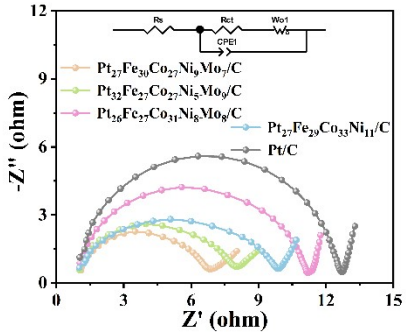

Figure S5. Nyquist plots of catalysts for HER at a potential of 0.00 V vs. RHE.

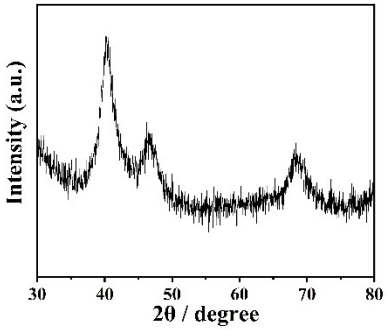

Figure S6. XRD spectrum of $Pt_{27}Fe_{30}Co_{27}Ni_9Mo_7/C$ catalyst after more than 40000s stability of hydrogen evolution reaction.

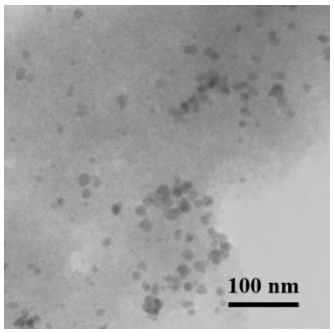

Figure S7. TEM image of $Pt_{27}Fe_{30}Co_{27}Ni_9Mo_7$/C catalyst after more than 40000s stability of hydrogen evolution reaction.

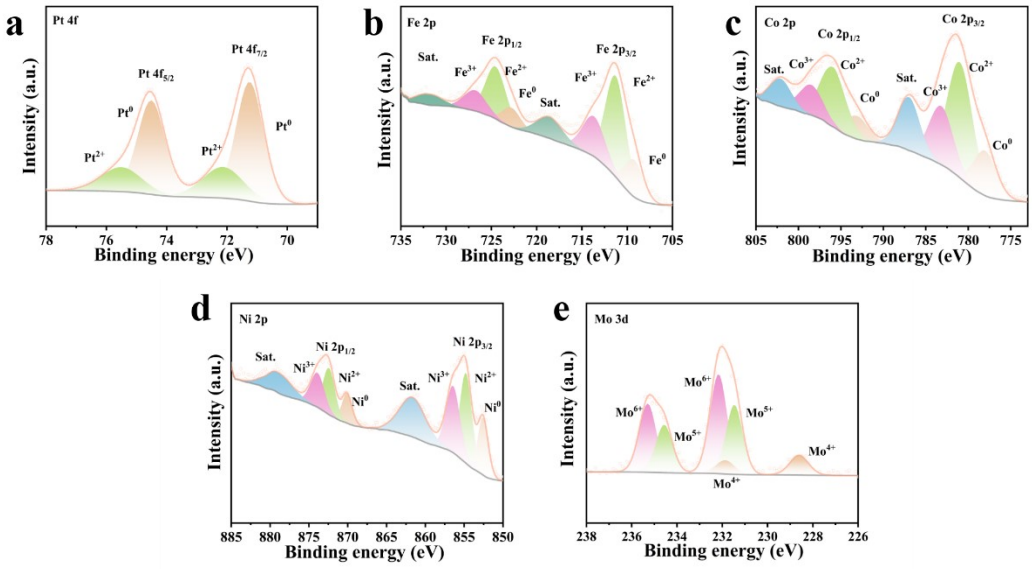

Figure S8. High-resolution XPS spectra of Pt 4f (a), Fe 2p (b), Co 2p (c), Ni 2p (d), and Mo 3d (e) in $Pt_{27}Fe_{30}Co_{27}Ni_9Mo_7$/C after HER.

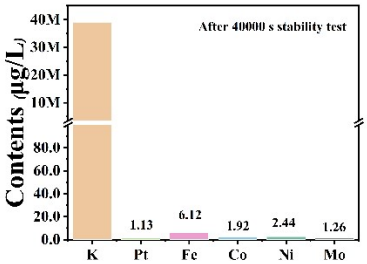

Fig.S9 The ICP-OES results of $Pt_{27}Fe_{30}Co_{27}Ni_9Mo_7$/C after 40000 s stability test confirm that only trace elements are dissolved.

Table S1. ICP-OES results of the contents of Pt, Fe, Co, Ni and Mo in HEA/C.

Catalysts	Elements (atomic rate%)				
	Pt	Fe	Co	Ni	Mo
$Pt_{27}Fe_{30}Co_{27}Ni_9Mo_7/C$	27.40	29.65	26.86	9.06	6.85
$Pt_{32}Fe_{27}Co_{27}Ni_5Mo_9/C$	31.54	26.96	26.78	5.26	9.46
$Pt_{26}Fe_{27}Co_{31}Ni_8Mo_8/C$	26.11	27.23	30.72	8.10	7.84
$Pt_{27}Fe_{29}Co_{33}Ni_{11}/C$	26.56	29.49	33.02	10.93	

Table S2. ICP-OES results of the contents of Pt, Fe, Co, Ni and Mo in HEA/C.

Catalysts	Elements (wt%)				
	Pt	Fe	Co	Ni	Mo
$Pt_{27}Fe_{30}Co_{27}Ni_9Mo_7/C$	3.66	1.13	1.08	0.36	0.45
$Pt_{32}Fe_{27}Co_{27}Ni_5Mo_9/C$	6.63	1.62	1.70	0.33	0.98
$Pt_{26}Fe_{27}Co_{31}Ni_8Mo_8/C$	3.02	0.90	1.07	0.28	0.45
$Pt_{27}Fe_{29}Co_{33}Ni_{11}/C$	3.84	1.22	1.44	0.48	

Table S3. The mixing enthalpy (ΔH_{mix}), mixing entropy (ΔS_{mix}), free energy (ΔG_{mix}), and atomic radius difference of each alloy.

Catalysts	ΔH_{mix} ($kJ \cdot mol^{-1}$)	ΔS_{mix} ($J \cdot K^{-1} \cdot mol^{-2}$)	ΔG_{mix}($kJ \cdot mol^{-1}$)	δ
$Pt_{27}Fe_{30}Co_{27}Ni_9Mo_7/C$	-5.98	12.22	-11.52	2.63
$Pt_{32}Fe_{27}Co_{27}Ni_5Mo_9/C$	-5.49	12.04	-10.95	2.90
$Pt_{26}Fe_{27}Co_{31}Ni_8Mo_8/C$	-5.87	12.23	-11.41	2.77
$Pt_{27}Fe_{29}Co_{33}Ni_{11}/C$	-4.90	10.97	-9.87	1.36

Table S4. Results of three parallel ICP-OES tests on $Pt_{27}Fe_{30}Co_{27}Ni_9Mo_7$/C catalysts.

Number	Elements (wt%)				
	Pt		Fe	Co	Ni
1	3.66	1.14	1.10	0.36	0.46
2	3.68	1.13	1.09	0.34	0.44
3	3.64	1.12	1.07	0.37	0.48

Table S5. The double-layer capacitance (C_{dl}), the electrochemically active surface area (ECSA) difference of each catalyst.

Catalysts	C_{dl} (mF cm^{-2})	ECSA (m^2/g)
$Pt_{27}Fe_{30}Co_{27}Ni_9Mo_7/C$	7.30	182.50
$Pt_{32}Fe_{27}Co_{27}Ni_5Mo_9/C$	5.43	135.75
$Pt_{26}Fe_{27}Co_{31}Ni_8Mo_8/C$	5.67	141.75
$Pt_{27}Fe_{29}Co_{33}Ni_{11}/C$	5.09	127.25
Pt/C	7.65	191.25

Table S6. Corresponding parameter of EIS for HER. The parameter of R_s, R_{ct}, and W_o for the electrocatalysts for HER.

Catalysts	R_s (Ω)	R_{ct} (Ω)	W_o (Ω)
$Pt_{27}Fe_{30}Co_{27}Ni_9Mo_7/C$	1.23	5.58	0.0011
$Pt_{32}Fe_{27}Co_{27}Ni_5Mo_9/C$	1.21	6.78	0.0038
$Pt_{26}Fe_{27}Co_{31}Ni_8Mo_8/C$	1.25	9.93	0.0047
$Pt_{27}Fe_{29}Co_{33}Ni_{11}/C$	1.24	7.59	0.0157
Pt/C	1.22	11.49	0.0015

Table S7. Comparison of HER performance of $Pt_{26}Ir_7Fe_{13}Co_{22}Ni_{32}$ NFs electrocatalyst with recently reported catalysts.

materials	Electrolyte	η10	Tafel slope	Ref.
		(10 mA cm^{-2})	(mV dec^{-1})	
$Pt_{27}Fe_{30}Co_{27}Ni_9Mo_7$/C	1.0 M KOH	24	48.44	This work
PtNiCuMnMo	1.0 M KOH	21	74	[4]
FeCoNiMnRu	1.0 M KOH	37	44	[5]
$Ni_3ZnC_{0.7}$@$NiPt_1$/NPC	1.0 M KOH	23	28.45	[6]
$Pt_{58}Cu_{15}Ni_{27}$	1.0 M KOH	30	40	[7]
FeCoNiMnRuLa/CNT	1.0 M KOH	50	116.9	[8]
$Pt_{26}Ir_7Fe_{13}Co_{22}Ni_{32}$NF	1.0 M KOH	26	44.5	[1]
$Rh_{2.6}Fe_3Co_{2.6}$@NG	1.0 M KOH	25	29.8	[9]
FeCoNiCrPt@Pt	1.0 M KOH	51	52.9	[10]
$Ti_{37}Cu_{60}Ru_3$	1.0 M KOH	35	34	[11]
PtNiMg	1.0 M KOH	22	30.9	[12]
FeCoNiCuMo	1.0 M KOH	60.1	33.4	[13]
PtFeCoNiCuCr@HCS	1.0 M KOH	29	39.24	[14]
PtAuPdRhRu NPs	1.0 M KOH	$190_{30\ mA\ cm-2}$	91	[15]
$(FeCoNiB_{0.75})_{97}Pt_3$	1.0 M KOH	27	/	[16]
PtPdRhRuCu HEA	1.0 M KOH	23.2	124	[17]
IrPdPtRhRu	1.0 M KOH	16	31	[18]
PtPdRhRuCu	1.0 M KOH	10	87	[19]
FeCoNiCuPd	1.0 M KOH	29.7	47.2	[20]

References

1. X. Ma, Y. Zhou, S. Zhang, W. Lei, Y. Zhao and C. Shan, *Small*, 2025, **21**, 2411394.
2. Z. Lu, W. Sun, P. Cai, L. Fan, K. Chen, J. Gao, H. Zhang, J. Chen and Z. Wen, *Energy & Environmental Science*, 2025, **18**, 2918-2930.
3. X. Ma, Y. Zhou, S. Zhang, W. Lei, Y. Zhao and C. Shan, *Small*, 2025, **21**, 2411394.
4. T. Gu, F. Yu, Z. Yu, Y. Qi, Y. Li, F. Miao and Z. Yan, *Journal of Colloid and Interface Science*, 2025, **688**, 308-316.
5. G. Liu, C. Song, X. Li, Q. Jia, P. Wu, Z. Lou, Y. Ma, X. Cui, X. Zhou and L. Jiang, *Chemical Engineering Journal*, 2025, **509**, 161070.
6. Y. Miao, Y. Liu, Y. Xu, J. Yang, J. Lan, Y. Yan, J. Ma, S. Sang, J. Zhou and M. Wang, *Nano Research*, 2025, **18**, 94907913.
7. I. Baldan Isik, Z. Eroglu, D. Kaya, F. Karadag, A. Ekicibil and O. Metin, *Rare Metals*, 2025, DOI: 10.1007/s12598-025-03579-2.
8. J. Chen, O. E. Onah, Y. Cheng, K. J. Silva, C. H. Choi, W. Chen, S. Xu, L. Eddy, Y. Han and B. I. Yakobson, *Small Methods*, 2025, **9**, 2400680.
9. A. Jiang, J. Chen, S. Liu, Z. Wang, Q. Li, D. Xia and M. Dong, *ACS Applied Nano Materials*, 2021, **4**, 13716-13723.
10. A. Hojjati-Najafabadi, R. Behmadi, Y. He, H. Kamyab and Y. Vasseghian, *Sustainable Materials and Technologies*, 2025, e01655.
11. J. Tian, Y. Hu, W. Lu, J. Zhu, X. Liu, J. Shen, G. Wang and J. Schroers, *Carbon Energy*, 2023, **5**, e322.
12. Y. Zheng, P. Shang, F. Pei, G. Ma, Z. Ye, X. Peng and D. Li, *Chemical Engineering Journal*, 2022, **433**, 134571.
13. S. Wang, H. Yan, W. Huo, M. Abdellatief, F. Fang and P. H. Camargo, *ACS Applied Materials & Interfaces*, 2025, **17**, 53587-53599.
14. Y. Wan, W. Wei, S. Ding, L. Wu, H. Qin and X. Yuan, *Advanced Functional Materials*, 2025, **35**, 2414554.
15 M. Liu, Z. Zhang, F. Okejiri, S. Yang, S. Zhou, S. Dai, *Adv. Mater. Interfaces* 2019, **6**, 1900015.
16 X. Zhang, Y. Yang, Y. Liu, Z. Jia, Q. Wang, L. Sun, L.-C. Zhang, J. J. Kruzic, J. Lu, B. Shen, *Adv. Mater.* 2023, **35**, 2303439.
17 G. Zhao, K. Lu, Y. Li, F. Lu, P. Gao, B. Nan, L. Li, Y. Zhang, P. Xu, X. Liu, L. Chen, *Chin. J. Catal.* 2024, **62**, 156.
18 Y. Yu, Q. Wang, X. Li, Q. Xie, K. Xu, S. Zhang, H. Zhang, M. Gong, W. Lei,

Nano Mater. Sci. 2024, DOI: https://doi.org/10.1016/j.nanoms.2024.05.012.

19 Y. Kang, O. Cretu, J. Kikkawa, K. Kimoto, H. Nara, A. S. Nugraha, H. Kawamoto, M. Eguchi, T. Liao, Z. Sun, T. Asahi, Y. Yamauchi, *Nat. Commun.* 2023, **14**, 4182.

20 S. Wang, B. Xu, W. Huo, H. Feng, X. Zhou, F. Fang, Z. Xie, J. K. Shang, J. Jiang, *Appl. Catal., B.,* 2022, **313**, 121472.